

**Tectonic
geomorphology at
small catchment
sizes**

S. Hergarten et al.

Tectonic geomorphology at small catchment sizes – extensions of the stream-power approach and the χ method

S. Hergarten¹, J. Robl², and K. Stüwe³

¹Institut für Geo- und Umweltnaturwissenschaften, Albert-Ludwigs-Universität Freiburg, Freiburg i. Br., Germany

²Institut für Geographie und Geologie, Universität Salzburg, Salzburg, Austria

³Institut für Erdwissenschaften, NAWI Graz, Karl-Franzens-Universität Graz, Graz, Austria

Received: 28 July 2015 – Accepted: 29 July 2015 – Published: 17 August 2015

Correspondence to: S. Hergarten (stefan.hergarten@geologie.uni-freiburg.de)

Published by Copernicus Publications on behalf of the European Geosciences Union.

Title Page

Abstract

Introduction

Conclusions

References

Tables

Figures

◀

▶

◀

▶

Back

Close

Full Screen / Esc

Printer-friendly Version

Interactive Discussion



Abstract

Quantitative tectonic geomorphology hinges on the analysis of longitudinal river profiles. The model behind almost all approaches in this field originates from an empirical relationship between channel slope and catchment size, often substantiated in form of the stream-power model for fluvial incision. A significant methodological progress was recently achieved by introducing the χ transform. It defines a nonlinear length coordinate in such a way that the inherent curvature of river profiles due to the increase of catchment sizes in downstream direction is removed from the analysis. However, the limitation to large catchment sizes inherited from the stream power approach for fluvial incision persists. As a consequence, only a small fraction of all nodes of a DEM can be used for the analysis. In this study we present and discuss some empirically derived extensions of the stream power law towards small catchment sizes in order to overcome this limitation. Beyond this, we introduce a simple method for estimating the adjustable parameters in the original χ method as well as in our extended approaches. As a main result, an approach originally suggested for debris flow channels seems to be the best approximation if both large and small catchment sizes are included in the same analysis.

1 Introduction

The vast majority of the approaches used to derive information on tectonic processes from topography is based on the analysis of longitudinal river profiles. The fundamental relationship between channel slope S and upstream catchment size A ,

$$S = k_s A^{-\theta}, \quad (1)$$

that is used to infer such information, dates back to a seminal empirical study of Hack (1957) and is often referred to as Flint's law (Flint, 1974). The parameters k_s and θ are denoted steepness index and concavity index, respectively.

ESURFD

3, 689–714, 2015

Tectonic geomorphology at small catchment sizes

S. Hergarten et al.

Title Page

Abstract

Introduction

Conclusions

References

Tables

Figures

◀

▶

◀

▶

Back

Close

Full Screen / Esc

Printer-friendly Version

Interactive Discussion



Understanding and quantitative interpretation of Eq. (1) hinges on the stream-power approach (e.g., Howard, 1994; Whipple and Tucker, 1999; Whipple, 2004; Wobus et al., 2006) where it is assumed that the rate of fluvial erosion in a bedrock channel depends on the product $A^\theta S$. In this context, Eq. (1) reflects a constant erosion rate along the river as it occurs, e.g., in equilibrium with homogeneous uplift.

In the simplest version of the stream-power approach it is assumed that the erosion rate E is linearly proportional to $A^\theta S$. The more general approach implements a power-law relationship

$$E = K \left(\left(\frac{A}{A_0} \right)^\theta S \right)^n, \quad (2)$$

where K is denoted erodibility. The arbitrary reference catchment size A_0 has been introduced as a scaling parameter in order to avoid an odd physical dimension of K . Using this scaling, K describes the erosion rate at a catchment size A_0 and a (hypothetical) channel slope of one. Although called erodibility, K does not only refer to the properties of the channel bed, but also contains the effect of precipitation as the erosion rate in principle depends on the discharge instead of the catchment size.

Physically based models of bedrock incision suggest that the concavity index θ of a steady-state bedrock river under homogeneous conditions does not only depend on the constitutive laws of the erosion process, but also on the cross-sectional geometry of the channels (e.g., Whipple, 2004; Whipple et al., 2013; Lague, 2014). This explains some variation in θ around the value $\theta \approx 0.5$ originally found by Hack (1957) or around the reference value $\theta_{\text{ref}} = 0.45$ being widely assumed for perfect bedrock channels under homogenous steady-state conditions (Whipple et al., 2013; Lague, 2014).

A range of θ between about 0.4 and 0.7 has been found under relatively homogeneous conditions (e.g., Whipple, 2004; Whipple et al., 2013), while apparent values significantly outside this range may arise from spatial inhomogeneity or non-steady topography. Analyzing channel slopes at constant catchment sizes, Hergarten et al. (2010) found a strong positive correlation between surface elevation and slope in sev-

Tectonic geomorphology at small catchment sizes

S. Hergarten et al.

Title Page

Abstract

Introduction

Conclusions

References

Tables

Figures



Back

Close

Full Screen / Esc

Printer-friendly Version

Interactive Discussion



eral orogens, suggesting a correlation between uplift rate and elevation. This correlation will lead to a higher apparent steepness index when following individual rivers, which may explain why the majority of the values of θ found in nature are greater than $\theta_{\text{ref}} = 0.45$.

5 Compared to the concavity index θ , less is known about the exponent n as it cannot be determined from individual equilibrium river profiles under uniform conditions. According to Eq. (4), the exponent n can be determined by comparing river segments being in equilibrium with different uplift rates, and the results tentatively suggest that n should not be far away from one (Wobus et al., 2006).

10 Using Eq. (2), the evolution of the surface elevation $H(x, t)$ along the stream profile through time under a given uplift rate U follows the partial differential equation

$$\frac{\partial H}{\partial t} = U - K \left(\left(\frac{A}{A_0} \right)^\theta \frac{\partial H}{\partial x} \right)^n, \quad (3)$$

where the linear coordinate x follows the upstream direction of the considered river. Both U and K may vary spatially and temporally.

15 The simplest interpretation of Eq. (3) refers to steady-state topography where uplift and erosion are in local equilibrium. Under these conditions, the ratio of uplift rate and erodibility can be directly obtained from the steepness index (Eq. 1) according to

$$\frac{U}{K} = \left(\frac{k_s}{A_0^\theta} \right)^n. \quad (4)$$

20 The most interesting applications of the stream-power erosion equation (Eq. 3), however, concern nonequilibrium river profiles due to temporally changing uplift rates or due to climate-induced changes in the erodibility. If such changes are discontinuous, they result in distinct knickpoints propagating in upstream direction.

**Tectonic
geomorphology at
small catchment
sizes**

S. Hergarten et al.

Title Page

Abstract

Introduction

Conclusions

References

Tables

Figures

◀

▶

◀

▶

Back

Close

Full Screen / Esc

Printer-friendly Version

Interactive Discussion



2 The χ transformation and its limitation

Recently, the so-called χ plot (or χ transformation) introduced the perhaps most important methodic progress in evaluating and interpreting longitudinal river profiles since the seminal work of Howard (1994). It transforms the upstream coordinate x to a new coordinate χ in such a way that the inherent curvature of equilibrium profiles due to the reduction of catchment size in upstream direction vanishes. The catchment size A can be eliminated from Eq. (3) if the transformation satisfies the condition

$$\frac{dx}{d\chi} = \left(\frac{A}{A_0} \right)^\theta, \quad (5)$$

which can be achieved by

$$\chi(x) = \int_{x_0}^x \left(\frac{A(\xi)}{A_0} \right)^{-\theta} d\xi, \quad (6)$$

where x_0 is an arbitrary reference point. As a result, the erosion rate (Eq. 2) is directly related to the slope of the river profile (H vs. χ),

$$E = K \left(\frac{\partial H}{\partial \chi} \right)^n, \quad (7)$$

and Eq. (3) simplifies to

$$\frac{\partial H}{\partial t} = U - K \left(\frac{\partial H}{\partial \chi} \right)^n. \quad (8)$$

The solutions of this equation and their potential for unraveling the uplift and erosion history have been discussed by Royden and Perron (2013), and a formal inversion procedure for the linear case ($n = 1$) has been presented by Goren et al. (2014).

Tectonic geomorphology at small catchment sizes

S. Hergarten et al.

Title Page

Abstract

Introduction

Conclusions

References

Tables

Figures

◀

▶

◀

▶

Back

Close

Full Screen / Esc

Printer-friendly Version

Interactive Discussion



The most striking property of the χ transformation is immediately recognized in Eq. (8): if U and K are spatially homogeneous, all upstream paths starting from x_0 are described by the same differential equation, so that the H vs. χ curves of all tributaries must collapse with the H vs. χ curve of the main stream. Conversely, spatial inhomogeneity results in a deviation of the curves belonging to different branches that increases in upstream direction. Thus, a narrow bunch of H vs. χ curves with a nonlinear overall shape is the fingerprint of temporal variations under spatially homogeneous conditions, while a wide, but overall straight bunch points towards spatial heterogeneity under steady-state conditions. This simple interpretation, however, only holds as long as the drainage pattern has not changed in the past since changes in catchment sizes also result in deviations between different branches (Willett et al., 2014; Yang et al., 2015).

Since a clear distinction requires the consideration of a large number of tributaries, the inherent limitation of the stream-power approach to the fluvial regime also limits the χ method. As addressed in several studies, Flint's law (Eq. 1) and thus the stream-power erosion equation (Eq. 2) with a constant concavity index θ breaks down at small catchment sizes where lower limits between about 0.1 and 5 km² have been reported (Montgomery and Foufoula-Georgiou, 1993; Stock and Dietrich, 2003; Wobus et al., 2006).

The transition from a fluvial regime at large catchment sizes to a regime dominated by hillslope processes is explored by an example from Taiwan in Fig. 1. Based on the recently released SRTM1 DEM with a mesh width of 1 arcsecond, flow directions (D8 algorithm, O'Callaghan and Mark, 1984), catchment sizes, and channel slopes were computed for the entire island after filling all local depressions. The mean slope (black markers) follows Eq. (1) well above some square kilometers catchment size with a steepness index $\theta_{\text{ref}} = 0.45$. Clear deviations from this behavior are visible at catchment sizes below about 2 km² in the Taiwan dataset. On the other hand, the number of nodes with a catchment size of A or larger roughly decreases like $A^{-0.5}$ (Maritan et al., 1996). For a DEM with a mesh width of 1 arcsecond, this means that

only some 2 % of all DEM nodes have a catchment size $A \geq 2 \text{ km}^2$, so that about 98 % of all nodes cannot be used in the χ method here.

3 Extending the χ method to small catchment sizes

In the following we present two extensions of the basic relationship between channel slope and catchment size (Eq. 1) towards small catchment sizes and their implementation in the χ method. In most applications of the χ method, the concavity index θ is considered as an adjustable parameter and used to improve either the straightness of the H vs. χ plot or the collinearity with tributaries. In the following, the approach with adjustable concavity index θ is denoted χ_θ , while χ represents the version with the reference value $\theta_{\text{ref}} = 0.45$. However, the curvature of the data in Fig. 1 already suggests that the adjustment of θ may only introduce a limited improvement at small catchment sizes compared to the reference value θ_{ref} .

The approaches presented in the following are intended to be as simple as possible. First, we aim at a representation by a uniform equation without distinguishing different regimes, although the domain below (concerning catchment size, but spatially above) the region where Flint's law holds is sometimes described as the debris flow regime (Stock and Dietrich, 2003). Second, it shall involve as few parameters as possible in order to limit the numerical effort of parameter estimation.

The data shown in Fig. 1 suggest that the erosion rate still depends on the catchment size at least for $A \geq 0.01 \text{ km}^2$, but this dependence is weaker than predicted by the stream-power law. A simple modification of Eq. (1) consists in adding a constant value a to the catchment size, i.e., to assume

$$S = k_s(A + a)^{-\theta}. \quad (9)$$

Tectonic geomorphology at small catchment sizes

S. Hergarten et al.

Title Page

Abstract

Introduction

Conclusions

References

Tables

Figures

⏪

⏩

◀

▶

Back

Close

Full Screen / Esc

Printer-friendly Version

Interactive Discussion



The respective modification of the χ transformation is

$$\chi_a(x) = \int_{x_0}^x \left(\frac{A(\xi) + a}{A_0} \right)^{-\theta} d\xi. \quad (10)$$

This extension can be either considered as a one-parametric approach where a is an adjustable parameter, while $\theta = \theta_{\text{ref}}$ is pre-defined, but also as a two-parametric approach with both a and θ being free parameters. For consistency, the latter is denoted $\chi_{\theta a}$ in the following.

As an alternative approach, a constant value can be added to the term A^θ . In order to avoid odd physical dimensions, this term is written in the form b^θ where b has the dimension of an area. With this extension, Eq. (1) turns into

$$S = \frac{k_s}{A^\theta + b^\theta}, \quad (11)$$

and the erosion rate (Eq. 2) becomes

$$E = K \left(\frac{A^\theta + b^\theta}{A_0^\theta} S \right)^n. \quad (12)$$

In the linear case ($n = 1$), this extension can be interpreted as an erosion rate consisting of two additive components being both proportional to the channel slope. One of them depends on the catchment size according to the stream-power law, while the second one is independent of the catchment size and may correspond, e.g., to hillslope erosion.

Equation (11) is essentially the same as the empirical relationship

$$S = \frac{s_0}{1 + a_1 A^{a_2}} \quad (13)$$

**Tectonic
geomorphology at
small catchment
sizes**

S. Hergarten et al.

Title Page

Abstract

Introduction

Conclusions

References

Tables

Figures

◀

▶

◀

▶

Back

Close

Full Screen / Esc

Printer-friendly Version

Interactive Discussion



Tectonic geomorphology at small catchment sizes

S. Hergarten et al.

Title Page

Abstract

Introduction

Conclusions

References

Tables

Figures

◀

▶

◀

▶

Back

Close

Full Screen / Esc

Printer-friendly Version

Interactive Discussion



pensated by smaller θ values here, the significant bias towards smaller θ values found for χ_θ is not surprising. In return, the two-parametric approach $\chi_{\theta a}$ exhibits a tendency towards values $\theta > \theta_{\text{ref}}$, reflected in median of $\theta = 0.56$. The other two-parametric approach, $\chi_{\theta b}$, yields best-fit θ values with a median of $\theta = 0.47$ close to the reference value $\theta_{\text{ref}} = 0.45$. While $\chi_{\theta a}$ and $\chi_{\theta b}$ are evenly matched with respect to the χ disorder on average, $\chi_{\theta a}$ obviously needs artificially increased θ values for achieving the best fit. The approach $\chi_{\theta b}$ turns out to be more robust against this bias, although some tendency towards larger θ values occurs if the catchment sizes are restricted to a narrower range (here, $1 \text{ km}^2 \leq A \leq 100 \text{ km}^2$). Under this aspect, the approach $\chi_{\theta b}$ should be superior to $\chi_{\theta a}$ if a wide range of catchment sizes is taken into account.

5 Conclusions

We have presented and investigated several concepts of extending Flint's law and the χ method towards small catchment sizes. Including points with small catchment sizes into the analysis of stream profiles strongly increases the data density and thus allows for a better distinction between effects temporal changes in uplift rate or climate and spatial heterogeneity.

Among the approaches considered in this study, an extension of Flints's law similar to an equation originally suggested for debris flow channels (Stock and Dietrich, 2003) turned out to be the most suitable concept if a wide range of catchment sizes is included. The respective definition of the extended χ transform (Eq. 14) can be implemented either as a two-parametric approach where both θ and b are adjustable parameters as well as a one-parametric approach where b is variable and $\theta = \theta_{\text{ref}}$ with $\theta_{\text{ref}} = 0.45$ or any other fixed reference value.

Minimizing the χ disorder defined in Eq. (17) provides a simple way to determine the best values of the adjustable parameters. It refers to the collinearity of tributaries and does not require any further assumptions such as spatial homogeneity or an uplift

rate being constant over distinct time intervals and should thus be applicable in a wide context.

References

- 5 Flint, J. J.: Stream gradient as a function of order, magnitude, and discharge, *Water Resour. Res.*, 10, 969–973, doi:10.1029/WR010i005p00969, 1974. 690
- Goren, L., Fox, M., and Willett, S. D.: Tectonics from fluvial topography using formal linear inversion: theory and applications to the Inyo Mountains, California, *J. Geophys. Res.-Earth*, 119, 1651–1681, doi:10.1002/2014JF003079, 2014. 693
- 10 Hack, J. T.: Studies of longitudinal profiles in Virginia and Maryland, no. 294-B in *US Geol. Survey Prof. Papers*, US Government Printing Office, Washington, DC, 1957. 690, 691
- Hergarten, S., Wagner, T., and Stüwe, K.: Age and prematurity of the Alps derived from topography, *Earth Planet. Sc. Lett.*, 297, 453–460, 2010. 691, 702
- Howard, A. D.: A detachment-limited model for drainage basin evolution, *Water Resour. Res.*, 30, 2261–2285, doi:10.1029/94WR00757, 1994. 691, 693
- 15 Lague, D.: The stream power river incision model: evidence, theory and beyond, *Earth Surf. Proc. Land.*, 39, 38–61, doi:10.1002/esp.3462, 2014. 691
- Maritan, A., Rinaldo, A., Rigon, R., Giacometti, A., and Rodriguez-Iturbe, I.: Scaling laws for river networks, *Phys. Rev. E*, 53, 1510–1515, 1996. 694
- 20 Montgomery, D. R. and Foufoula-Georgiou, E.: Channel network source representation using digital elevation models, *Water Resour. Res.*, 29, 3925–3934, doi:10.1029/93WR02463, 1993. 694
- Mudd, S. M., Attal, M., Milodowski, D. T., Grieve, S. W. D., and Valters, D. A.: A statistical framework to quantify spatial variation in channel gradients using the integral method of channel profile analysis, *J. Geophys. Res.-Earth*, 119, 138–152, doi:10.1002/2013JF002981, 2014. 698
- 25 O'Callaghan, J. F. and Mark, D. M.: The extraction of drainage networks from digital elevation data, *Comput. Vision Graph.*, 28, 323–344, 1984. 694
- Ono, Y., Aoki, T., Hasegawa, H., and Dali, L.: Mountain glaciation in Japan and Taiwan at the global Last Glacial Maximum, *Quatern. Int.*, 138–139, 79–92, doi:10.1016/j.quaint.2005.02.007, 2005. 699
- 30

Tectonic geomorphology at small catchment sizes

S. Hergarten et al.

Title Page

Abstract

Introduction

Conclusions

References

Tables

Figures



Back

Close

Full Screen / Esc

Printer-friendly Version

Interactive Discussion



Tectonic geomorphology at small catchment sizes

S. Hergarten et al.

Title Page

Abstract

Introduction

Conclusions

References

Tables

Figures

◀

▶

◀

▶

Back

Close

Full Screen / Esc

Printer-friendly Version

Interactive Discussion



Perron, J. T. and Royden, L.: An integral approach to bedrock river profile analysis, *Earth Surf. Proc. Land.*, 38, 570–576, doi:10.1002/esp.3302, 2013. 697

Royden, L. and Perron, J. T.: Solutions of the stream power equation and application to the evolution of river longitudinal profiles, *J. Geophys. Res.-Earth*, 118, 497–518, doi:10.1002/jgrf.20031, 2013. 693

Stock, J. and Dietrich, W. E.: Valley incision by debris flows: evidence of a topographic signature, *Water Resour. Res.*, 39, 1089, doi:10.1029/2001WR001057, 2003. 694, 695, 697, 703

Whipple, K. X.: Bedrock rivers and the geomorphology of active orogens, *Annu. Rev. Earth Pl. Sc.*, 32, 151–185, doi:10.1146/annurev.earth.32.101802.120356, 2004. 691

Whipple, K. X. and Tucker, G. E.: Dynamics of the stream power river incision model: implications for height limits of mountain ranges, landscape response time scales and research needs, *J. Geophys. Res.*, 104, 17661–17674, doi:10.1029/1999JB900120, 1999. 691

Whipple, K. X., DiBiase, R. A., and Crosby, B. T.: Bedrock rivers, in: *Fluvial Geomorphology*, edited by: Shroder, J. and Wohl, E., vol. 9, *Treatise on Geomorphology*, Academic Press, San Diego, CA, 550–573, 2013. 691

Willett, S. D., McCoy, S. W., Perron, J. T., Goren, L., and Chen, C.-Y.: Dynamic reorganization of river basins, *Science*, 343, 1248765, doi:10.1126/science.1248765, 2014. 694

Wobus, C., Whipple, K. X., Kirby, E., Snyder, N., Johnson, J., Spyropoulou, K., Crosby, B., and Sheehan, D.: Tectonics from topography: procedures, promise, and pitfalls, in: *Tectonics, Climate, and Landscape Evolution*, edited by: Willett, S. D., Hovius, N., Brandon, M. T., and Fisher, D. M., *Geological Society of America*, Boulder, Washington, DC, USA, 55–74, doi:10.1130/2006.2398(04), 2006. 691, 692, 694

Yang, R., Willett, S. D., and Goren, L.: In situ low-relief landscape formation as a result of river network disruption, *Nature*, 520, 526–529, doi:10.1038/nature14354, 2015. 694

Tectonic geomorphology at small catchment sizes

S. Hergarten et al.

Title Page

Abstract

Introduction

Conclusions

References

Tables

Figures

◀

▶

◀

▶

Back

Close

Full Screen / Esc

Printer-friendly Version

Interactive Discussion

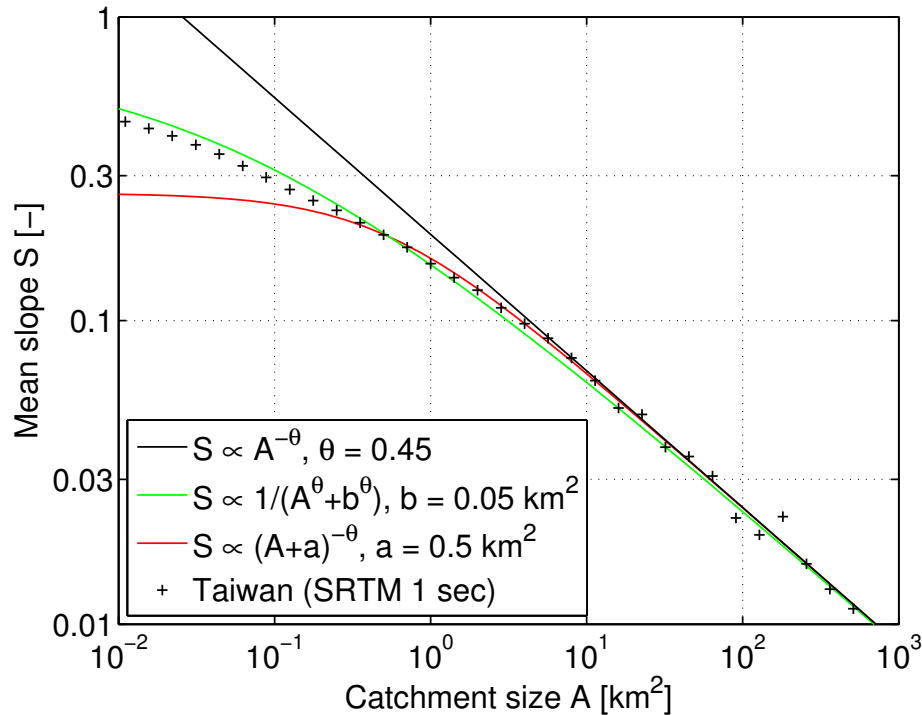


Figure 1. Relationship between mean channel slope and catchment size for the topography of Taiwan. Channel slopes and catchment sizes were derived from the SRTM1 DEM, and mean slopes were obtained from logarithmic bins with a factor $\sqrt{2}$ (black markers).

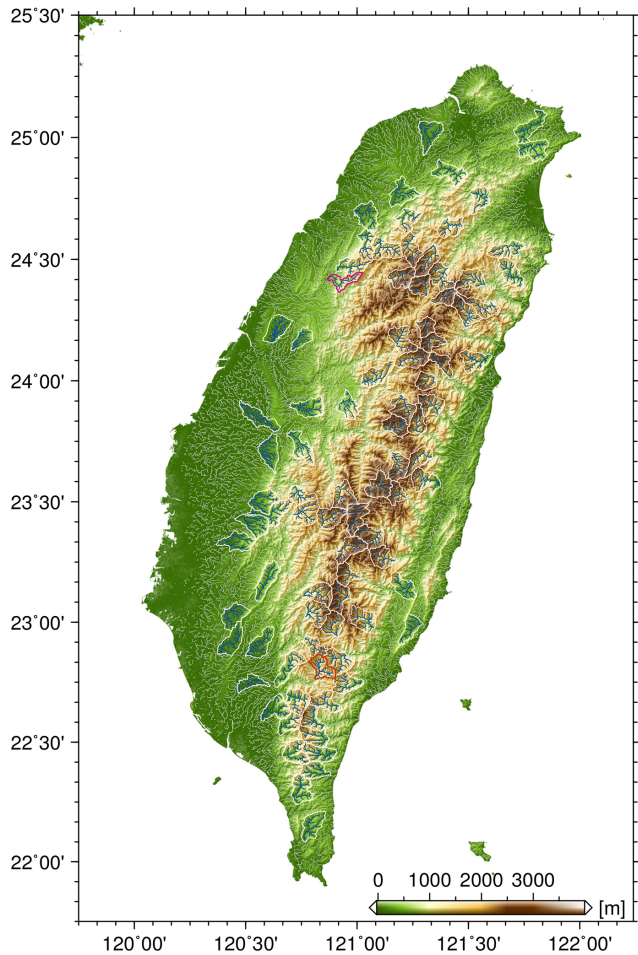


Figure 2. Map of the 89 considered catchments in Taiwan with catchment sizes $A \approx 100 \text{ km}^2$. The two catchments bordered in magenta and red are considered in detail in Figs. 4–6.

ESURFD

3, 689–714, 2015

Tectonic geomorphology at small catchment sizes

S. Hergarten et al.

Title Page

Abstract

Introduction

Conclusions

References

Tables

Figures



Back

Close

Full Screen / Esc

Printer-friendly Version

Interactive Discussion



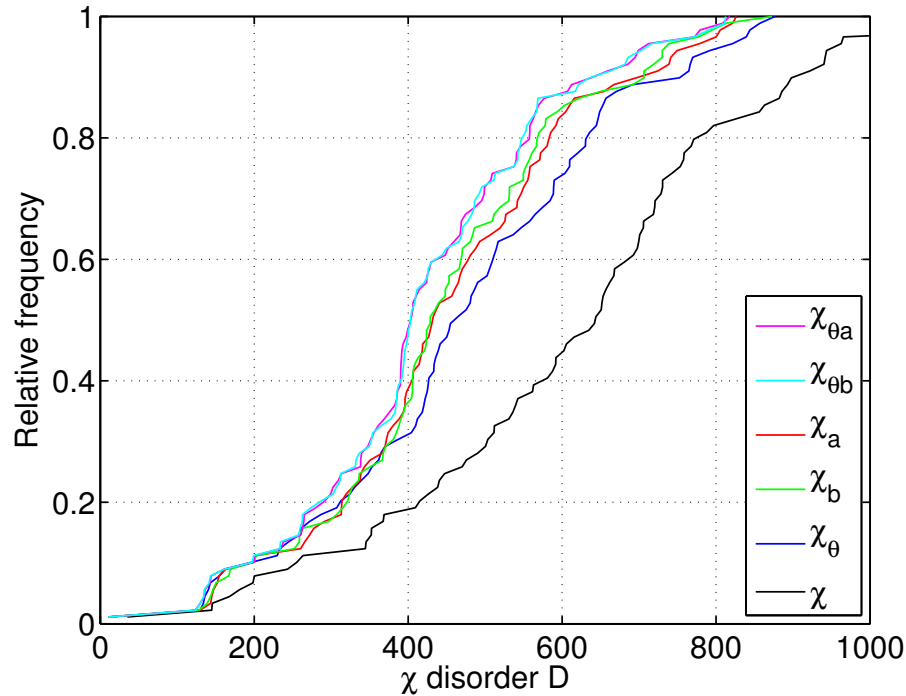


Figure 3. Cumulative distribution of the χ disorder for the 89 considered catchments in Taiwan for $0.01 \text{ km}^2 \leq A \leq 100 \text{ km}^2$. Each curve describes the relative number of the catchments with a χ disorder lower than or equal to the value D on the x axis.

**Tectonic
geomorphology at
small catchment
sizes**

S. Hergarten et al.

Title Page

Abstract Introduction

Conclusions References

Tables Figures

◀ ▶

◀ ▶

Back Close

Full Screen / Esc

Printer-friendly Version

Interactive Discussion



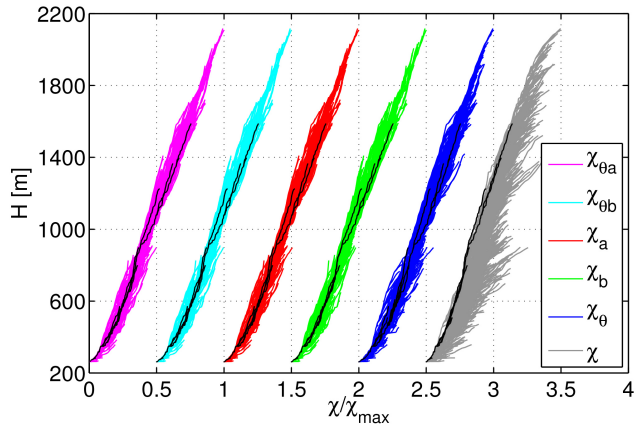
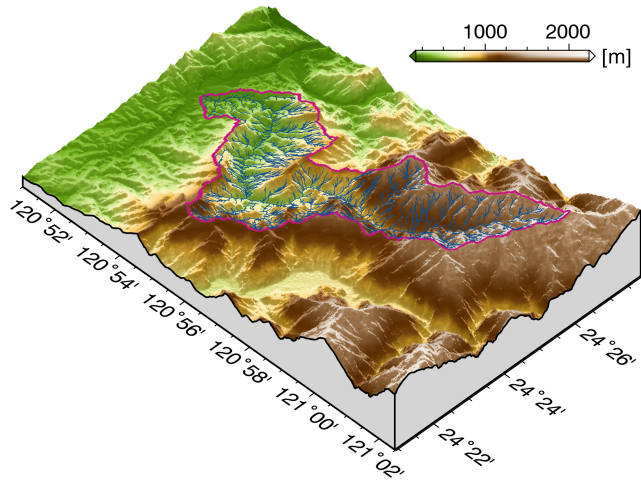


Figure 4. The mountainous catchment in Taiwan with the lowest χ disorder. The H vs. χ plots are shifted horizontally in order to avoid overlapping curves. The black lines show the part of the drainage network with $A \geq 1 \text{ km}^2$.

**Tectonic
geomorphology at
small catchment
sizes**

S. Hergarten et al.

Title Page

Abstract

Introduction

Conclusions

References

Tables

Figures

◀

▶

◀

▶

Back

Close

Full Screen / Esc

Printer-friendly Version

Interactive Discussion



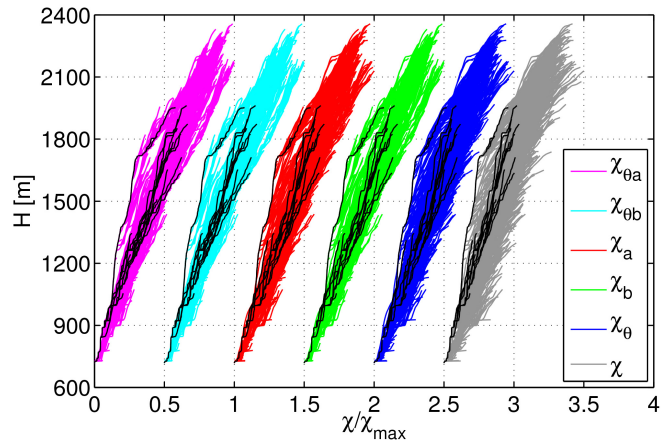
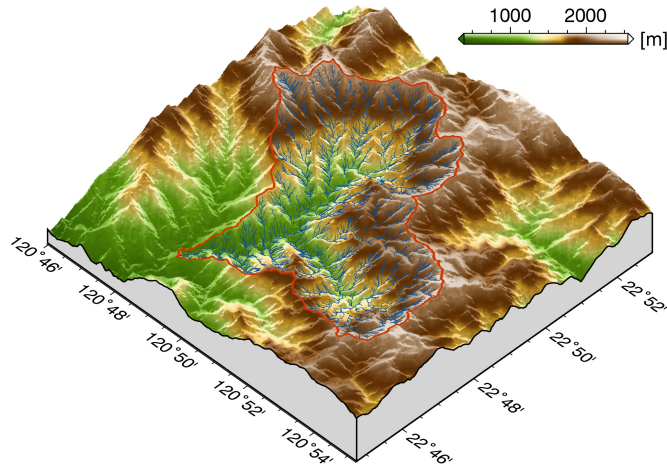


Figure 5. A catchment in Taiwan with a rather high χ disorder. The H vs. χ plots are shifted horizontally in order to avoid overlapping curves. The black lines show the part of the drainage network with $A \geq 1 \text{ km}^2$.

**Tectonic
geomorphology at
small catchment
sizes**

S. Hergarten et al.

Title Page

Abstract

Introduction

Conclusions

References

Tables

Figures

◀

▶

◀

▶

Back

Close

Full Screen / Esc

Printer-friendly Version

Interactive Discussion



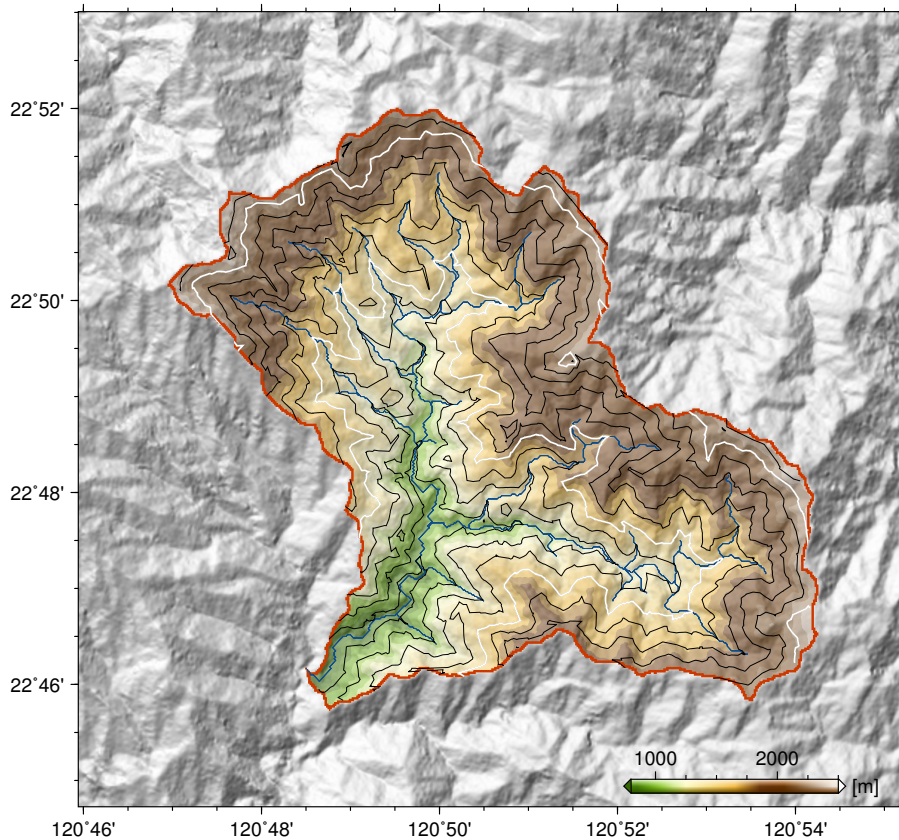


Figure 6. Map of elevation (encoded by colors) and $\chi_{\theta b}$ values (contour lines) of the catchment considered in Fig. 5. The contour line interval is 0.5 km, and the lines of $\chi_{\theta b} = 2.5$ km and $\chi_{\theta b} = 5$ km are emphasized by white color.

Tectonic geomorphology at small catchment sizes

S. Hergarten et al.

Title Page

Abstract

Introduction

Conclusions

References

Tables

Figures



Back

Close

Full Screen / Esc

Printer-friendly Version

Interactive Discussion



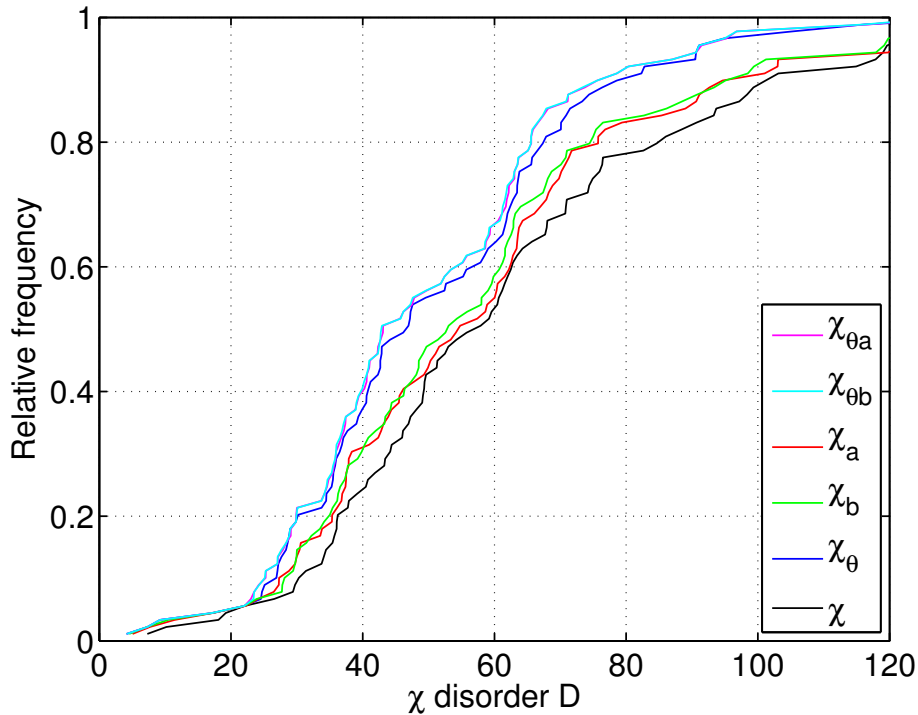


Figure 7. Cumulative distribution of the χ disorder for the 89 considered catchments in Taiwan for $1 \text{ km}^2 \leq A \leq 100 \text{ km}^2$. Each curve describes the relative number of the catchments with a χ disorder lower than or equal to the value D on the x axis.

**Tectonic
geomorphology at
small catchment
sizes**

S. Hergarten et al.

Title Page

Abstract Introduction

Conclusions References

Tables Figures

◀ ▶

◀ ▶

Back Close

Full Screen / Esc

Printer-friendly Version

Interactive Discussion



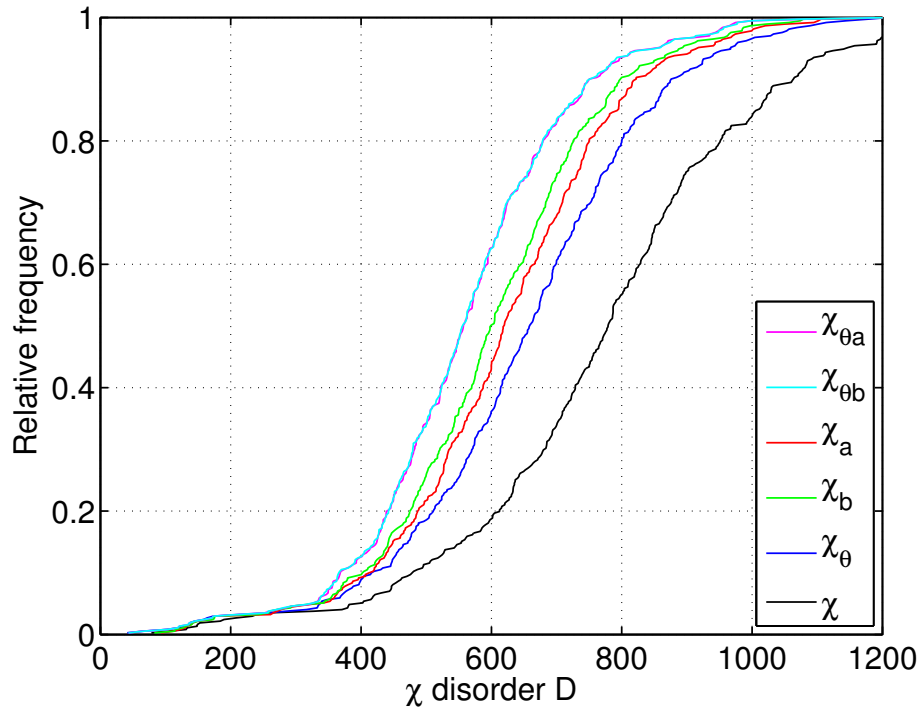


Figure 8. Cumulative distribution of the χ disorder for the 371 considered catchments in the European Alps for $0.01 \text{ km}^2 \leq A \leq 100 \text{ km}^2$. Each curve describes the relative number of the catchments with a χ disorder lower than or equal to the value D on the x axis.

**Tectonic
geomorphology at
small catchment
sizes**

S. Hergarten et al.

Title Page	
Abstract	Introduction
Conclusions	References
Tables	Figures
◀	▶
◀	▶
Back	Close
Full Screen / Esc	
Printer-friendly Version	
Interactive Discussion	



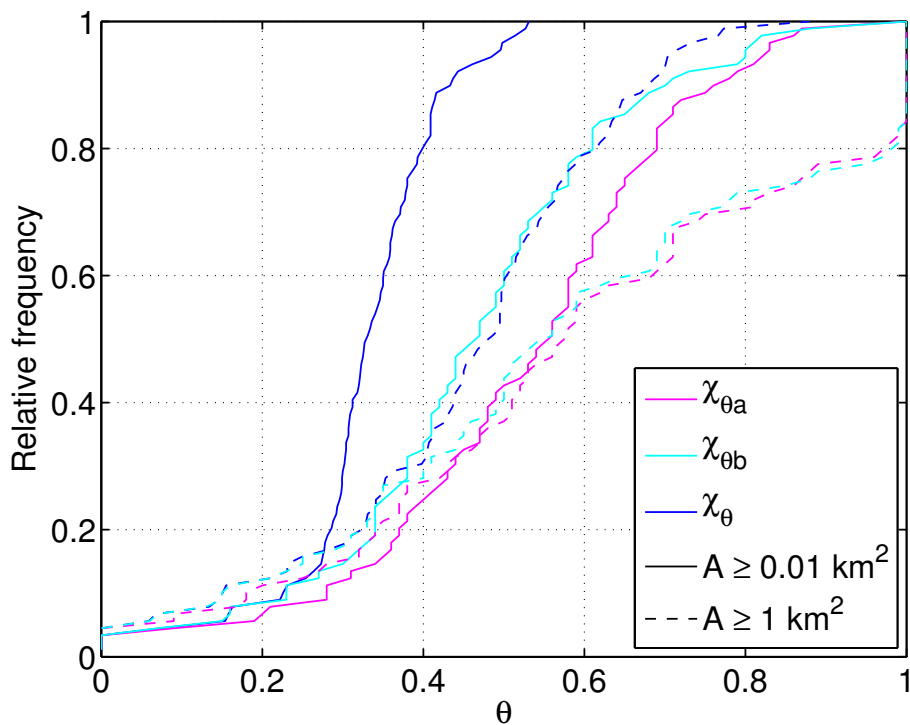


Figure 9. Cumulative distribution of the concavity index θ for the 89 considered catchments in Taiwan. Each curve describes the relative number of the catchments with an estimated concavity index lower than or equal to the value θ on the x axis. Solid lines refer to fits over the entire range $0.01 \text{ km}^2 \leq A \leq 100 \text{ km}^2$, while dashed lines correspond to fits for $A \geq 1 \text{ km}^2$ only.

**Tectonic
geomorphology at
small catchment
sizes**

S. Hergarten et al.

Title Page	
Abstract	Introduction
Conclusions	References
Tables	Figures
◀	▶
◀	▶
Back	Close
Full Screen / Esc	
Printer-friendly Version	
Interactive Discussion	

